AIP | Applied Physics Letters

A transparent 90° polarization rotator by combining chirality and electromagnetic wave tunneling

Mehmet Mutlu and Ekmel Ozbay

Citation: Appl. Phys. Lett. **100**, 051909 (2012); doi: 10.1063/1.3682591
View online: http://dx.doi.org/10.1063/1.3682591
View Table of Contents: http://apl.aip.org/resource/1/APPLAB/v100/i5
Published by the American Institute of Physics.

A transparent 90° polarization rotator by combining chirality and electromagnetic wave tunneling

Mehmet Mutlu[a] and Ekmel Ozbay
Department of Electrical and Electronics Engineering, Nanotechnology Research Center, Bilkent University, 06800 Ankara, Turkey

(Received 27 September 2011; accepted 19 January 2012; published online 3 February 2012)

A three-layer chiral metamaterial is constructed by using two layers of four mutually rotated resonators and a subwavelength mesh sandwiched symmetrically between these layers. The resulting structure is an ultrathin, transparent, and polarization angle independent 90° polarization rotator. Due to the electromagnetic tunneling effect exerted by the negative permittivity mesh, a cross-polarization conversion efficiency of 99% and 93% is achieved numerically and experimentally. The structure is modeled using the effective medium theory and then the transfer matrix method is applied to demonstrate the existence of the tunneling resonance theoretically. © *2012 American Institute of Physics*. [doi:10.1063/1.3682591]

A polarization rotator rotates the polarization plane of a linearly polarized electromagnetic (EM) wave by a fixed angle, while maintaining its linearly polarized nature. Conventional methods for building such devices require the usage of dextrorotatory and levorotatory crystals, the Faraday Effect, anisotropic media, and twisted nematic liquid crystals.[1] Such methods generally result in devices that have thicknesses comparable to the operation wavelength, which is an important drawback for low frequency applications. Metamaterials, which is a class of artificial media, have many intriguing properties[2–4] and as an alternative to the aforementioned methods, several metamaterial structures have recently been proposed in order to rotate the polarization plane of linearly polarized waves. Usage of metamaterials that exhibit optical activity removes the thickness problem as a result of being electrically thin. However, some drawbacks of these structures can be briefly listed as interference effects between the incident and reflected waves[5] and the polarization angle dependent response.[6–8] Afterwards, several other structures overcoming these drawbacks have been proposed in the literature.[9–12] However, these designs are not *transparent* to the incident waves such that they cannot transmit the incident field with *unit transmittance*. As a consequence, transmission losses still remain as an issue.

In the present paper, we report a three-layer and ultrathin chiral metamaterial that rotates the polarization plane of an incident linearly polarized wave by 90° with unit transmittance independent of the polarization angle. The governing physical mechanism for unit transmittance is the tunneling of EM waves through negative permittivity media with high magnetic fields.[13] This effect is predictable using the transfer-matrix method (TMM) and has been reported in the literature utilizing various other structures.[7,14–16] In order to determine the basic design steps for obtaining the desired response, the required transmission matrix for the structure is predicted using Jones calculus. It is assumed that the incident field is linearly polarized at an angle θ with respect to the x-axis. Using the Jones calculus formalism, the transmission matrix of a polarization independent 90° polarization rotator should satisfy the following equation:

$$\begin{pmatrix} T_{xx} & T_{xy} \\ T_{yx} & T_{yy} \end{pmatrix} \begin{pmatrix} \cos(\theta) \\ \sin(\theta) \end{pmatrix} = \begin{pmatrix} -\sin(\theta) \\ \cos(\theta) \end{pmatrix}, \tag{1}$$

where T_{xx}, T_{xy}, T_{yx}, and T_{yy} are the elements of the transmission matrix of the desired structure. The solution of Eq. (1) yields $T_{xx} = T_{yy} = 0$ and $T_{yx} = -T_{xy} = 1$. In order to design a structure by achieving the required transmission coefficients, the eigenvalues obtained from Eq. (1) are investigated. The eigenvalues of the matrix are given by the following equation:[17]

$$\kappa_{1,2} = \frac{1}{2}\left[(T_{xx} + T_{yy}) \pm \sqrt{(T_{xx} - T_{yy})^2 + 4T_{xy}T_{yx}}\right]. \tag{2}$$

In solving Eq. (2), the eigenvalues are obtained as $\pm i$. Using these eigenvalues, the normalized eigenbasis matrix is written as

$$\hat{\Lambda} = \frac{1}{\sqrt{2}} \begin{pmatrix} 1 & 1 \\ i & -i \end{pmatrix}. \tag{3}$$

This basis matrix is known to transform from the linear base to the circular base. From the given basis matrix, the normalized eigenvectors are obtained as

$$\vec{i}_1 = \frac{1}{\sqrt{2}} \begin{pmatrix} 1 \\ i \end{pmatrix}, \; \vec{i}_2 = \frac{1}{\sqrt{2}} \begin{pmatrix} 1 \\ -i \end{pmatrix}. \tag{4}$$

Equation (4) states that in order to obtain 90° polarization rotation for an incident wave that is linearly polarized at an arbitrary angle, the eigenwaves of the structure must be counter-rotating circularly polarized waves. Therefore, the utilization of a chiral metamaterial is a possible method for obtaining the desired response.[18] Transforming the desired transmission matrix to the circular base, the following transmission matrix is obtained:

$$\hat{T}_{circ} = \begin{pmatrix} T_{++} & T_{+-} \\ T_{-+} & T_{--} \end{pmatrix} = \begin{pmatrix} -i & 0 \\ 0 & i \end{pmatrix}. \tag{5}$$

[a]Electronic mail: mutlu@ee.bilkent.edu.tr.

Briefly, the structure should advance the phase of right-hand circularly polarized (RCP, +) waves by 90° while lagging the phase of the left-hand circularly polarized (LCP, −) waves by 90°. At the same time, the RCP and LCP components should be transmitted with unit transmittance for the achievement of the maximum cross-polarization conversion efficiency.

In the proposed design, an ABA stacking scheme in the circular base is utilized, where the combination AA forms the chiral metamaterial that is given in Ref. 11. It is noteworthy that the utilization of this specific chiral design is not mandatory for the purpose of achieving the desired transmission characteristics. In fact, any properly optimized chiral metamaterial that has C_4 symmetry can be utilized in the current approach. Layer B is a subwavelength mesh that exhibits negative effective permittivity throughout the investigated frequency range. The subwavelength mesh is positioned between the two A layers symmetrically without leaving an air gap as to form the composite structure. The three layers and the composite structure are depicted in Fig. 1. For layer B, the geometrical parameters are given by $w = 0.5$ mm and $p = 3.2$ mm. For layer A, the geometrical parameters are given by $s = 6$ mm, $g = 0.7$ mm, $d = 2$ mm. These parameters imply that the periodicity in the x and y directions is equal to 16 mm. As the substrate, teflon layers with a thickness of 1.2 mm, relative dielectric constant of 2.1, and a loss tangent of 0.0002 are utilized. For the metallic parts, copper with a thickness of 20 μm is used. Layer A is printed on the teflon and has a total thickness of 1.22 mm. For the experiment, layer B is printed on the backside of one of the A layers. However, in the theoretical calculations, it is considered to be a stand-alone structure with a thickness of 20 μm. Given beforehand that the operating frequency is 7 GHz, the electrical thickness of the composite structure corresponds to $\lambda/21$. The electrical thickness of the structure reveals that giant optical activity is achieved in an ultra-thin region. In addition, in the transverse plane, the periodicity in the x and y directions corresponds to 0.37λ.

We started the analysis with the numerical simulations using CST MICROWAVE STUDIO, a commercially available simulation software program that is based on the finite integration method. In the simulations, the boundary conditions along the x and y directions are adjusted to be periodic, whereas the absorbing boundary condition is applied for the z direction. Normally incident plane waves propagating in the $+z$ direction, are used for the excitation. In order to experimentally verify the operation of the proposed structure, we fabricated the structure with the dimension of 18 by 18 unit cells. The experiment is conducted using two standard horn antennas facing each other at a 60 cm distance. The measurements are performed using an Anritsu 37369 A network analyzer.

The numerical and experimental linear transmission coefficients are given in Figs. 2(a) and 2(b), respectively. As a result of the C_4 symmetry of the structure, it is obtained that $T_{xx} = T_{yy}$ and $T_{yx} = -T_{xy}$. Therefore, only T_{xx} and T_{yx} are discussed for simplicity. Numerical results show that in the vicinity of 7 GHz and 7.5 GHz, $|T_{xx}|$ is −42 dB and −60 dB, respectively. On the other hand, at these frequencies $|T_{yx}|$ is given as −0.04 dB and −17.5 dB. According to the numerical data, the cross-polarization conversion efficiency is 99% at 7 GHz and 2% at 7.5 GHz. In the experiment, $|T_{xx}|$ is measured to be −31 dB and −32 dB at 7 GHz and 7.5 GHz, respectively, whereas $|T_{yx}|$ is equal to −0.3 dB and −21 dB. As a result, an experimental cross-polarization conversion efficiency of 93% and 1% is achieved at 7 GHz and 7.5 GHz, respectively. For the purpose of achieving unit transmittance, the frequency of interest is 7 GHz and at this frequency, a low-loss and tunneling assisted mode is supported. Although the experimental efficiencies are lower than the numerical ones, the results obtained from the experiment are in good agreement with the simulations.

Using the eigenbasis matrix given in Eq. (3), under the four-fold rotational symmetry consideration, one can

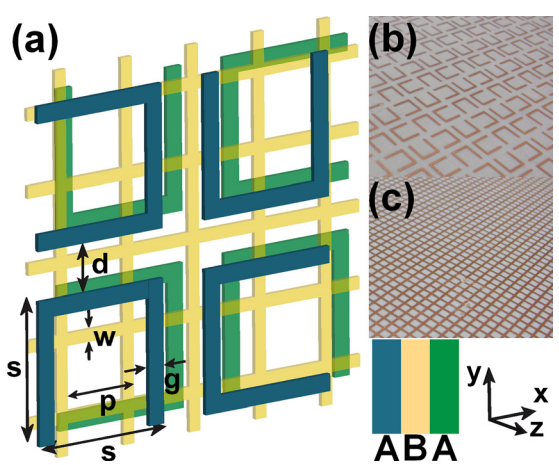

FIG. 1. (Color online) (a) Visual representation of the three-layer structure without teflon substrates. The color of each layer is different and the stacking scheme with respect to the colors is presented on the bottom-right corner. Photographs of the experimental sample for (b) layer A and (c) layer B.

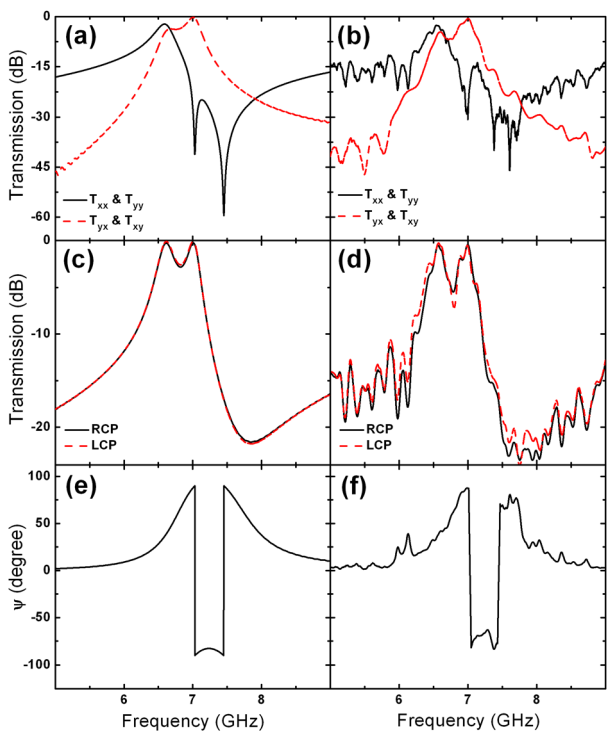

FIG. 2. (Color online) Numerical and experimental (a), (b) linear and (c), (d) circular transmission coefficients. (e), (f) The numerical and experimental polarization rotation angles.

calculate the transmission coefficients for RCP and LCP waves using $T_{\pm} = T_{xx} \mp iT_{yx}$. Accordingly, the numerical and experimental transmission coefficients for RCP and LCP waves are given in Figs. 2(c) and 2(d). Two peaks are observed in the transmission spectra of the RCP and LCP waves and these peaks will be investigated in the subsequent sections. At the frequency of interest, 7 GHz, numerical results state that the transmission of the RCP and LCP components are −0.05 dB and −0.03 dB, respectively. On the other hand, in the experiment, −0.36 dB and −0.26 dB are obtained for the RCP and LCP waves.

Afterwards, using the linear transmission coefficients, the polarization rotation azimuth angle ψ can be calculated as

$$\psi = \frac{1}{2}\tan^{-1}\left\{\frac{2R\cos(\varphi)}{1-R^2}\right\}, \quad (6)$$

where $R = |T_{yx}|/|T_{xx}|$and $\varphi = \angle T_{yx} - \angle T_{xx}$ (Ref. 1). Numerical and experimental results for the polarization rotation angle are shown in Figs. 2(e) and 2(f), respectively. Finally, the ellipticity χ of the transmitted waves is calculated as

$$\chi = \frac{1}{2}\sin^{-1}\left\{\frac{2R\sin(\varphi)}{1+R^2}\right\}. \quad (7)$$

As a result of using a very low loss substrate, the ellipticities of the transmitted waves are in the close vicinity of 0°. At 7 GHz, the numerical results state that ψ and χ are given by 90.1° and −0.5°, respectively. Experimental results agree closely with the simulations providing that ψ and χ are equal to 88.9° and −1.5° at the same frequency. Therefore, it is concluded that the transmitted waves are linearly polarized and the polarization planes of the incident waves are rotated by approximately 90° in transmission.

In order to describe the behavior of the proposed design theoretically, we employ the effective medium theory (EMT) formalism. Simulating the A and B layers individually and using the obtained complex transmission coefficients, we modeled the A and B layers as two homogenous dielectric slabs with $\varepsilon_A^{eff} = 1 + 172.7/(7.55^2 - f^2)$ and $\varepsilon_B^{eff} = 1.94 \ -47.2^2/f^2$, where f is the frequency in GHz. Since the individual layer A is achiral and assumed to be lossless, RCP and LCP eigenwaves experience the same effective permittivity in this layer, that is ε_A^{eff}. Layer B is also an achiral structure that exhibits identical effective permittivities for the RCP and LCP waves. As a result, the same effective permittivity values can be used in the calculation of the magnitudes of the two circular transmission coefficients. The effective thicknesses required to regenerate the numerically obtained magnitude and phase information are determined as 1.22 mm for layer A and 1.65 mm for layer B. The spectrum of the magnitude of the circular transmission coefficient, which is obtained using the TMM, is presented in Fig. 3. As a consequence of ignoring the losses in the calculations, the transmissions of the RCP and LCP waves are obtained to be identical. The peak at 7 GHz, which is numerically and experimentally verified, is reproduced by the TMM calculation supporting that the existence of this peak is a result of the electromagnetic wave tunneling effect.

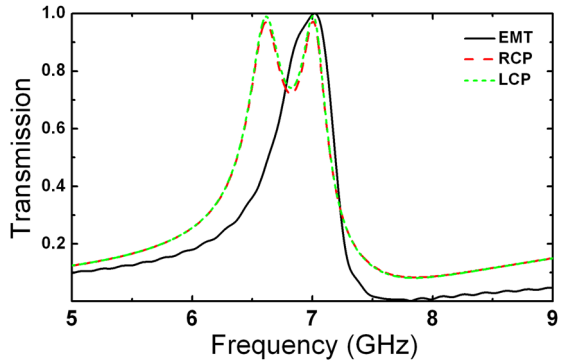

FIG. 3. (Color online) Comparison of the numerical circular transmission coefficients with the theoretically predicted transmission coefficient using TMM.

The peak at 6.5 GHz is not observed in the TMM prediction and, therefore, it is expected that this peak is a result of another physical mechanism. We predict that this peak is governed by the extraordinary transmission (EOT) phenomenon.[19] The effect of EOT is observed in Ref. 4 and described rigorously. Surface wave modes that normally lie below the light line can be excited due to the additional wavevector, G, that originates from the periodicity of layer A. We did not investigate the origin of this peak deeply since it is not a focus of this study. However, we added a 0.3 mm space between the layers in the simulations and observed that the peak at 6.5 GHz disappears, whereas the peak at 7 GHz still conforms to the TMM predictions. Therefore, we deduce that the peak at 6.5 GHz is strongly dependent on the dielectric/metal interface and most likely to be an EOT peak.

In conclusion, we have combined the giant optical activity effect arising due to chirality with the EM wave tunneling phenomenon to design an ultrathin, polarization independent, and transparent 90° polarization rotator. Using this tunneling assisted chirality mechanism, cross-polarization conversion is performed with almost 100% efficiency. Such devices can be employed in antenna applications, laser applications, remote sensors, and liquid crystal displays. Plus, the suggested approach and ideas for the current design may be adapted for the terahertz and optical applications.

This work is supported by the projects DPT-HAMIT, EU-PHOME, EU-N4E, and NATO-SET-181, and TUBITAK by the projects 107A004, 107A012, and 109E301. One of the authors (E.O.) also acknowledges partial support from the Turkish Academy of Sciences.

[1]B. E. A. Saleh and M. C. Teich, *Fundamentals of Photonics* (Wiley, New Jersey, 2007).
[2]D. R. Smith, W. J. Padilla, D. C. Vier, S. C. Nemat-Nasser, and S. Schultz, Phys. Rev. Lett. **84**, 4184 (2000).
[3]K. Aydin, I. Bulu, and E. Ozbay, Opt. Express **13**, 8753 (2005).
[4]N. Katsarakis, T. Koschny, M. Kafesaki, E. N. Economou, E. Ozbay, and C. M. Soukoulis, Phys. Rev. B **70**, 201101(R) (2004).
[5]J. Hao, Y. Yuan, L. Ran, J. A. Kong, C. T. Chan, and L. Zhou, Phys. Rev. Lett. **99**, 063908 (2007).
[6]J. Y. Chin, M. Lu, and T. J. Cui, Appl. Phys. Lett. **93**, 251903 (2008).
[7]W. Sun, Q. He, J. Hao, and L. Zhou, Opt. Lett. **36**, 927 (2011).
[8]T. Q. Li, H. Liu, T. Li, S. M. Wang, F. M. Wang, R. X. Wu, P. Chen, S. N. Zhu, and X. Zhang, Appl. Phys. Lett. **92**, 131111 (2008).
[9]Y. Ye and S. He, Appl. Phys. Lett. **96**, 203501 (2010).

[10]M. Liu, Y. Zhang, X. Wang, and C. Jin, Opt. Express **18**, 11990 (2010).
[11]X. Xiong, W. H. Sun, Y. J. Bao, M. Wang, R. W. Peng, C. Sun, X. Lu, J. Shao, Z. F. Li, and N. B. Ming, Phys. Rev. B **81**, 075119 (2010).
[12]R. Zhao, L. Zhang, J. Zhou, T. Koschny, and C. M. Soukoulis, Phys. Rev. B **83**, 035105 (2011).
[13]L. Zhou, W. Wen, C. T. Chan, and P. Sheng, Phys. Rev. Lett. **94**, 243905 (2005).
[14]B. Hou, H. Wen, Y. Leng, and W. Wen, Appl. Phys. Lett. **87**, 201114 (2005).
[15]G. Castaldi, I. Gallina, V. Galdi, A. Alu, and N. Engheta, Phys. Rev. B **83**, 081105(R) (2011).
[16]G. Castaldi, V. Galdi, A. Alu, and N. Engheta, J. Opt. Soc. Am. B **28**, 2362 (2011).
[17]C. Menzel, C. Rockstuhl, and F. Lederer, Phys. Rev. A **82**, 053811 (2010).
[18]B. Wang, J. Zhou, T. Koschny, M. Kafesaki, and C. M. Soukoulis, J. Opt. A, Pure Appl. Opt. **11**, 114003 (2009).
[19]T. W. Ebbesen, H. J. Lezec, H. F. Ghaemi, T. Thio, and P. A. Wolff, Nature **391**, 667 (1998).